Molecular Therapy
Nucleic Acids
Original Article

Long-Term PEDF Release in Rat Iris and Retinal Epithelial Cells after *Sleeping Beauty* Transposon-Mediated Gene Delivery

Laura Garcia-Garcia,[1,14] Sergio Recalde,[1,14] Maria Hernandez,[1,14] Jaione Bezunartea,[1] Juan Roberto Rodriguez-Madoz,[2] Sandra Johnen,[3] Sabine Diarra,[3] Corinne Marie,[4,5,6,7] Zsuzsanna Izsvák,[8] Zoltán Ivics,[9] Daniel Scherman,[4,5,6,7] Martina Kropp,[10,11] Gabriele Thumann,[10,11] Felipe Prosper,[2,12] Patricia Fernandez-Robredo,[1,15] and Alfredo Garcia-Layana[1,13,15]

[1]Experimental Ophthalmology Laboratory, University of Navarra, Navarra Institute for Health Research, IdiSNA, 31008 Pamplona, Spain; [2]Cell Therapy Program, Center for Applied Medical Research (CIMA), University of Navarra, Navarra Institute for Health Research, IdiSNA, 31008 Pamplona, Spain; [3]Department of Ophthalmology, University Hospital RWTH Aachen, Pauwelsstraße 30, 52074 Aachen, Germany; [4]CNRS, Unité de Technologies Chimiques et Biologiques pour la Santé (UTCBS) UMR 8258, 75006 Paris, France; [5]Université Paris Descartes, Sorbonne-Paris-Cité, UTCBS, 75006 Paris, France; [6]Chimie ParisTech, PSL Research University, UTCBS, 75005 Paris, France; [7]INSERM, UTCBS U 1022, 75006 Paris, France; [8]Max Delbrück Center for Molecular Medicine in the Helmholtz Society, 13125 Berlin, Germany; [9]Division of Medical Biotechnology, Paul Ehrlich Institute, 63225 Langen, Germany; [10]Experimental Ophthalmology, University of Geneva, 1205 Geneva, Switzerland; [11]Department of Ophthalmology, University Hospitals and School of Medicine, 22 Rue Alcide-Jentzer, Geneva 1205, Switzerland; [12]Area of Cell Therapy, Clínica Universidad de Navarra, University of Navarra, Navarra Institute for Health Research, IdiSNA, 31008 Pamplona, Spain; [13]Ophthalmology Department, Clínica Universidad de Navarra, 31008 Pamplona, Spain

Pigment epithelium derived factor (PEDF) is a potent antiangiogenic, neurotrophic, and neuroprotective molecule that is the endogenous inhibitor of vascular endothelial growth factor (VEGF) in the retina. An ex vivo gene therapy approach based on transgenic overexpression of PEDF in the eye is assumed to rebalance the angiogenic-antiangiogenic milieu of the retina, resulting in growth regression of choroidal blood vessels, the hallmark of neovascular age-related macular degeneration. Here, we show that rat pigment epithelial cells can be efficiently transfected with the PEDF-expressing non-viral hyperactive *Sleeping Beauty* transposon system delivered in a form free of antibiotic resistance marker miniplasmids. The engineered retinal and iris pigment epithelium cells secrete high (141 ± 13 and 222 ± 14 ng) PEDF levels in 72 hr in vitro. In vivo studies showed cell survival and insert expression during at least 4 months. Transplantation of the engineered cells to the subretinal space of a rat model of choroidal neovascularization reduces almost 50% of the development of new vessels.

INTRODUCTION

Elevated levels of vascular endothelial growth factor (VEGF) have been linked to the development of several ocular pathologies, including neovascular age-related macular degeneration (nAMD) and diabetic retinopathy.[1] VEGF is a potent endothelial mitogen and vascular permeability factor and is considered the principal driver of choroidal neovascularization (CNV).[2] The appropriate balance between the pro-angiogenic VEGF and the anti-angiogenic pigmented epithelium-derived factor (PEDF) in the retina could be essential to prevent the development of CNV.[3] PEDF was first identified in retinal pigment epithelial (RPE) cells, but it is expressed in many cell types in the eye. In addition to a potent antiangiogenic effect, PEDF has neurotrophic and neuroprotective properties.[4] The current treatment for neovascular retinal diseases is the inhibition of VEGF, specifically by the intravitreal injection of ranibizumab, the Fab fragment of a humanized antibody against VEGF (Lucentis, Novartis Pharma, Basel, Switzerland), aflibercept, a recombinant fusion protein (Eylea, Bayer Plc, UK), or bevacizumab, the whole humanized antibody against VEGF (Avastin, Roche, Basel, Switzerland). The injection of these anti-VEGFs controls CNV in nAMD patients, and in 30%–40% of cases, improves vision significantly.[2,5–8] However, effective treatment requires frequent, costly,[9,10] and life-long intraocular injections, and can be associated with side effects, such as endophthalmitis, ocular hypertension, and retinal detachment.[11,12]

To avoid life-long, frequent intraocular injections, long-term delivery systems, e.g., nanoparticles,[13] have been studied to transfer plasmids with the therapeutic gene. Likewise, many different antiangiogenic molecules are under study, such as sFLT01,[14] Flt23K,[15] or angiopoietin-1.[16]

Received 3 October 2016; accepted 7 August 2017;
http://dx.doi.org/10.1016/j.omtn.2017.08.001.

[14]These authors contributed equally to this work.

[15]These authors contributed equally to this work.

Correspondence: Patricia Fernandez-Robredo, Experimental Ophthalmology Laboratory, University of Navarra, Navarra Institute for Health Research, IdiSNA, 31008 Pamplona, Spain.
E-mail: pfrobredo@unav.es

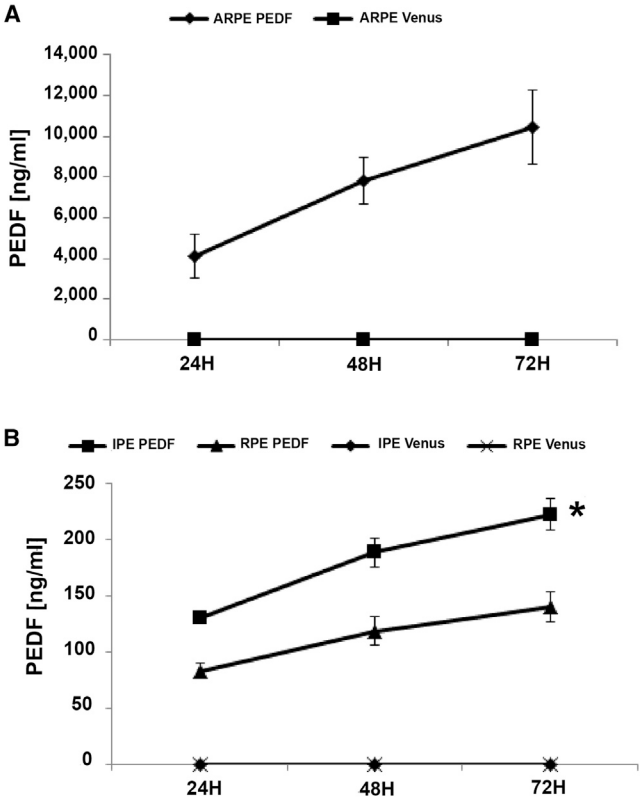

Figure 1. PEDF Quantification

Total PEDF secreted by cells seeded was quantified by ELISA every 24 hr. (A) PEDF produced by ARPE-19 cells. (B) PEDF secreted by RPE and IPE cells. There was no detectable PEDF in control Venus-transfected samples. Data are presented as mean ± SEM (n = 5). *p < 0.05.

The delivery of anti-angiogenic factors to the retina using gene therapy could be approached by the direct administration[17] or transplantation of ex vivo engineered RPE cells expressing anti-angiogenic factors.[18] In a number of cases, the gene is delivered using adeno-associated virus (AAV) vectors; however, the required re-administration may compromise efficacy[19] and might induce an immune response. Recent clinical studies showed that intravitreal sFLT01[20] and subretinal endostatin/angiostatin[21] injections seemed to be safe and well tolerated, although the efficacy in the CNV reduction was not confirmed. The *Sleeping Beauty* (*SB*) system that we proposed has a reduced immunogenicity,[22] improved safety/toxicity profiles,[23,24] and a relaxed limitation on the size of expression cassettes.[25,26] We combined the non-viral hyperactive *SB* (*SB100X*) transposon system and the pFAR4 vector (free of antibiotic resistance genes) to deliver the *PEDF* gene to pigment epithelial cells. We transplant the ex vivo engineered, PEDF-expressing cells subretinally. Both the *SB100X* transposase and the *PEDF* gene are carried by pFAR4 derivatives. We hypothesized that we could provide efficient gene delivery, sustained gene expression, as well as improved biosafety by avoiding the potential transfer of antibiotic resistance genes into the host cell. The transposon-mediated integration of the *PEDF* gene into pigment epithelial cells would result in the continuous expression of the PEDF that would then inhibit the further development or even regression of CNV.[24,27,28]

Here, we report on the efficient transfection of rat RPE and iris pigment epithelial cells (IPEs) with the *PEDF* gene using the *SB100X* transposon system delivered by pFAR4 plasmids, the sustained release of recombinant PEDF in vitro, the proper localization of transfected cell transplanted subretinally, and the inhibition of neovascularization in a rat model of CNV.

RESULTS

PEDF Production by ARPE-19 and Rat Primary IPE and RPE Cells Transfected with the *PEDF* Gene

Before transfection with the *SB* transposon vector expressing PEDF, cells were characterized to confirm that they retained their expected phenotype in culture (Figure S1). ARPE-19 cells (Figures S1A–S1I) were positive for RPE65 and CRALBP, primary RPE cells (Figures S1J–S1O) were positive for RPE65 and Bestrophin, and IPE cells reacted positively for cytokeratin 18 (CK18) (Figures S1P–S1R). Quantification by ELISA detected continuous secretion of PEDF in the engineered ARPE-19, primary RPE, and IPE cells over a 72-hr period (Figures 1A and 1B). Importantly, PEDF secretion was increased from 24 to 72 hr in all three cell types (Figures 1A and 1B), reaching significance for IPE cells ($p = 0.011$). ARPE-19 cells secreted approximately 50-fold more PEDF than IPE or RPE primary cells did (10,434 ± 1,820 ng/mL secreted by ARPE-19 and 141 ± 13 ng/mL and 222 ± 14 ng/mL secreted by RPE and IPE cells, respectively). There was no detectable PEDF in control Venus-transfected samples.

PEDF secretion in vitro was maintained over 8 weeks for the three cell types studied (Figure 2) when transfected with PEDF and *SB100X*. A very significant change in PEDF levels was detected in IPE cells ($p < 0.01$). These results are in accordance with the ones obtained in previous studies.[28]

In addition to PEDF, a His-tagged version of *PEDF* (*PEDF-His*) was also transfected into ARPE-19, RPE, and IPE cells. Both forms of PEDF were easily detectable, as illustrated by western blots of culture supernatants of ARPE-19, RPE, and IPE cells (Figure 3).

Localization of Transplanted Venus-Transfected Cells in the Subretinal Space

Engineered Venus reporter-expressing cells were transplanted into the subretinal space of the rat. Cell localization of transplanted cells was assessed in flat mount retinas and cross-section cryosections of eyes 7 days after transplantation (Figures 4 and S2). Importantly, Venus-positive cells were located mostly around the site of injection (Figures 4A–4D). Flat mount images showed cells transfected with Venus and labeled with CellBrite to confirm that the Venus-positive cells were the ones injected (Figures 4E–4L). In addition, flat mounts of the RPE/choroid complex observed by confocal microscopy showed that the Venus-transplanted cells were located close to the

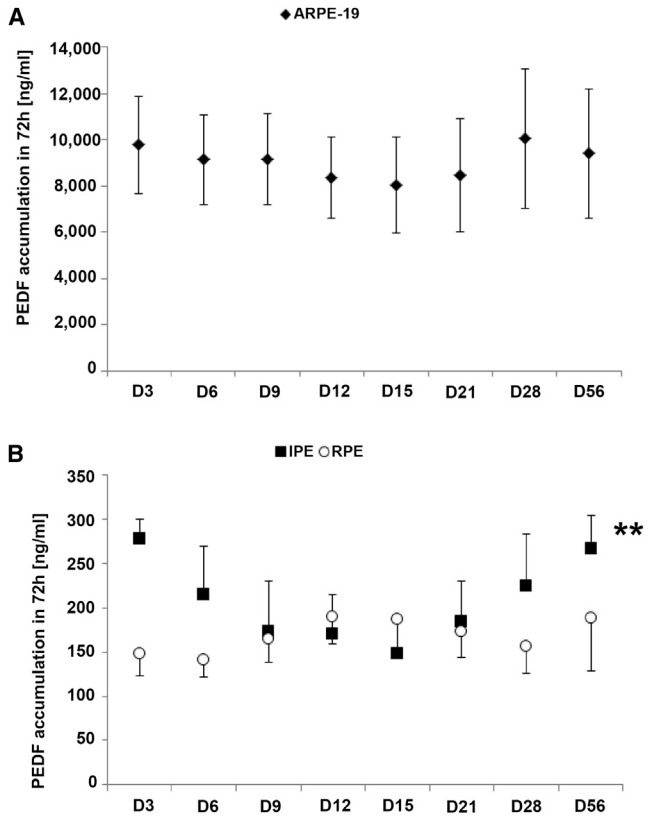

Figure 2. PEDF Detection in the Supernatants during 8 Weeks

PEDF secretion accumulated during 72 hr was measured by ELISA at different time points (days 3, 6, 9, 12, 15, 21, 28, and 56). (A and B) Diagrams show PEDF accumulation in ARPE-19 cells (A) and RPE and IPE cells (B). Data are presented as mean ± SEM (n = 3). **p < 0.01.

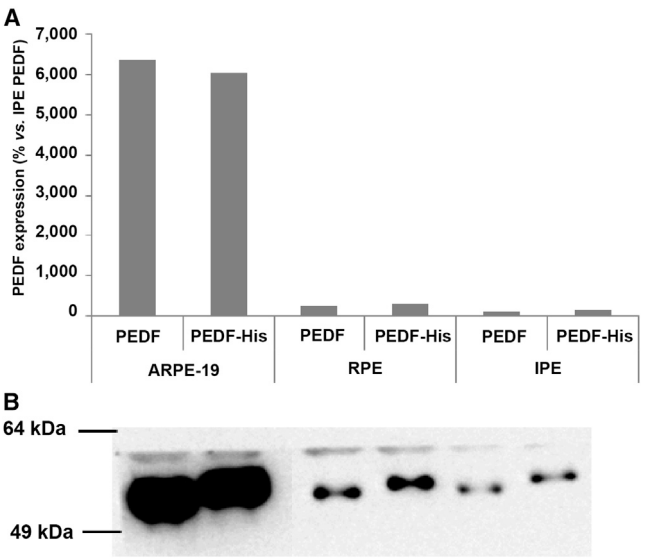

Figure 3. PEDF and PEDF-His Secretion by Western Blot

Analysis of ARPE-19, RPE, and IPE cells' supernatants. Both plasmids were able to transfect cells and produce the protein of interest with a similar efficiency. (A) Densitometric analysis of PEDF detection. (B) Image of PEDF detection by western blot (WB).

tight junctions (labeled with ZO-1) of the native RPE, as illustrated in the orthogonal stack image (Figure S3).

Venus-transfected cells were stained with CellBrite and transplanted into the subretinal space. Inmunostaining for RPE65 was done, but transplanted RPE cell staining was not clear, as described by Petrus-Reurer et al.[29] (Figure 5). CellBrite marked organelles and the cytoplamic membrane of cells, and it confirmed that Venus-positive cells were the transplanted cells, even if they were not positive for RPE65.

The correct location of transfected cells was also verified in eye samples transplanted with 1,000 IPE or RPE cells (Figure 6) transfected with Venus and previously stained with CellBrite. These samples showed the location of RPE (Figures 6A–6I) and IPE (Figures 6J–6W) cell clusters 1 week after transplantation.

PEDF-His production was tested 2 weeks after the transplantation. Confocal analysis of retinal flat mounts stained with antibodies to PEDF and 6-His peptide showed that the transplanted IPE cells were alive and produced PEDF-His in the subretinal space (Figure S4A). The orthogonal projections confirmed localization of the injected cells in the subretinal space (Figure S4B).

Transfected Cells Survive Long-Term in the Subretinal Space

Cell survival was evaluated in flat mounts of retinas from rats transplanted with Venus-transfected rat IPE and RPE primary cells. In the flat mounts, both RPE- and IPE-Venus-positive cells were detected at 7 days, 14 days, and 4 months after transplantation (Figure 7). In addition, a Z-orthogonal image showed the correct location in the subretinal space of the RPE-transplanted cells for 4 months (Figure S5).

In Vivo Efficacy Study

The effect of PEDF secretion was monitored 12 days after laser-CNV induction and 10 days post-subretinal transplantation of PEDF-expressing primary cells. The CNV area was stained with caveolin-1 antibody. It is evident from the photomicrographs (Figure 8A) and the area of CNV quantification (Figure 8B) that the area of CNV is 41% in the three rats transplanted with 10,000 PEDF-expressing IPE cells and 46% in the three rats transplanted with 20,000 PEDF-expressing RPE cells compared to the area of CNV in rats injected with saline. By contrast, no difference in the CNV lesion size was detected in the four control groups (Figure 8C).

DISCUSSION

We have previously reported the stable and efficient transgene integration in bovine, human, and immortalized rat RPE cells transfected with *PEDF* gene using the *SB100X* transposon system.[28,30] Here, we show that ARPE-19 or rat primary RPE and IPE cells can be transfected by the PEDF expression construct using the *SB100X* transposase, both

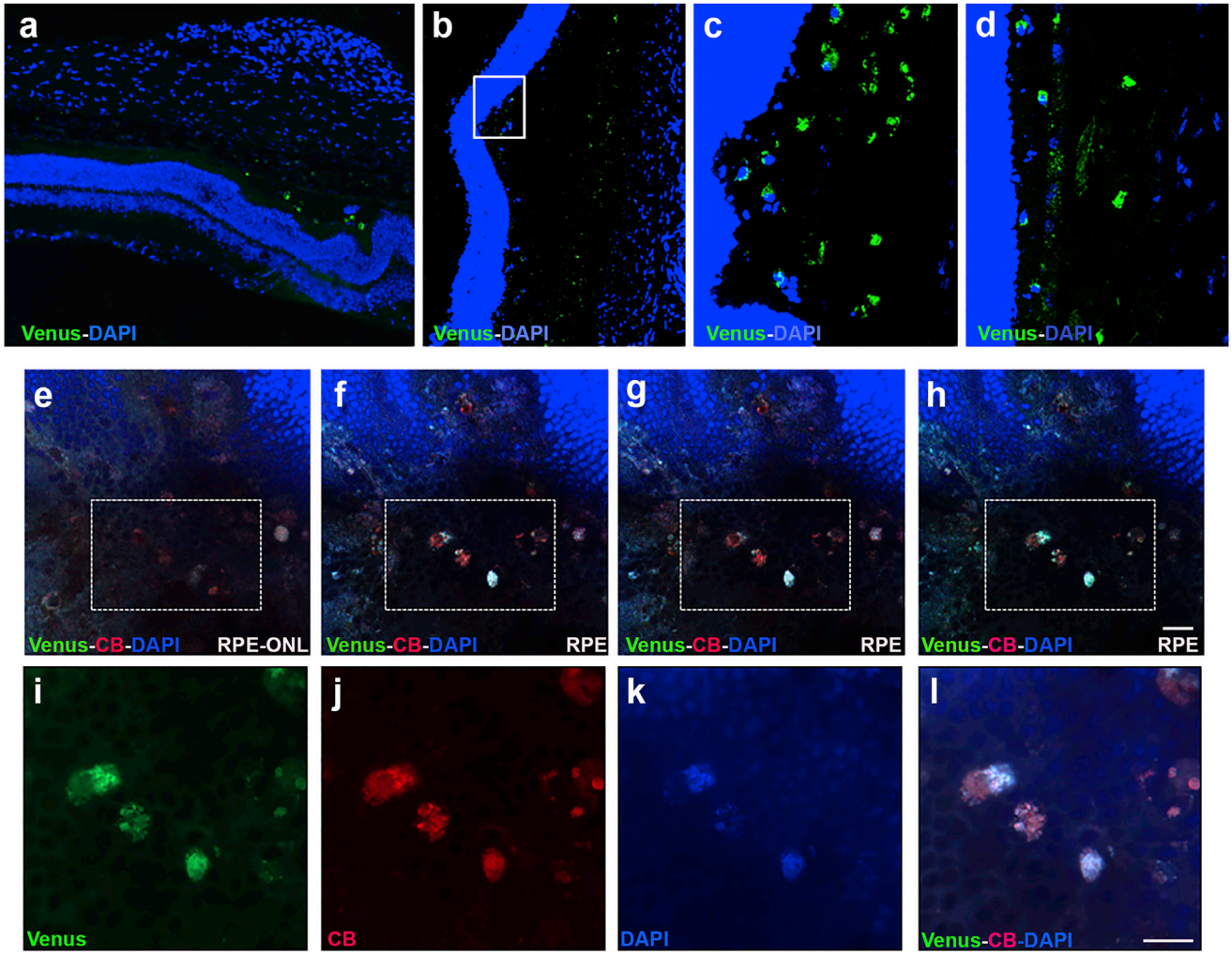

Figure 4. Distribution of the Primary Cells Injected

Representative images of the primary cells in the subretinal space. (A) Cross retinal section showing Venus-positive cells near to the photoreceptor layer at the site of injection. (B–D) Cross sectional retinal areas injected with primary cells transfected with Venus (scale bar, 100 μm). (E–H) Flat mount retinas injected with rat RPE cells transfected with Venus (green) and labeled with CellBrite (red) and DAPI (blue) from ONL (E) to RPE (F–H). (I–L) The highlighted with rectangles were examined at higher magnification with confocal super-resolution imaging. CellBrite labeled the plasmatic membrane and DAPI labeled the nuclei. Scale bar, 50 μm. CB, CellBrite; RPE, retinal pigment epithelium; ONL, outer nuclear layer.

encoded in pFAR miniplasmids. Cells secrete PEDF for at least 8 weeks into the culture media in vitro and 2 weeks transplanted subretinally. To our knowledge, this is the first demonstration that PEDF is expressed subretinally by *PEDF*-transfected primary cells for at least 2 weeks, and, as shown previously in similar studies,[30] the transplanted cells reduce neovascularization in a rat model of CNV. Likewise, Venus-transfected rat IPE and RPE cells produced Venus fluorescent protein in the subretinal space for at least 4 months after transplantation.

Because the use on anti-VEGFs for the treatment of neovascular AMD is effective in only 30%–40% of patients and because it is necessary that anti-VEGFs be injected intraocularly every 4–8 weeks for the life of the patient and because the treatment is costly[9,10] and may elicit significant side effects,[11,12,31,32] it is imperative that novel, long-lasting, and more effective treatments be discovered.[18] We have proposed the transplantation of *PEDF*-transfected pigment epithelial cells as a long-term alternative to the frequent intraocular injections of anti-VEGFs for the treatment for nAMD.

Given that gene delivery by viral vectors has significant limitations,[33] we have investigated the use of the non-viral *SB100X* coupled with pFAR miniplasmid technology. The *SB100X* transposon vector provides efficient integration of the therapeutic gene into the host cell's genome and sustained gene expression in many cell types,[34,35] including RPE and IPE cells,[28] as we report here. In addition, *Sleeping Beauty* is relatively safe because unlike integrating viral vectors, it

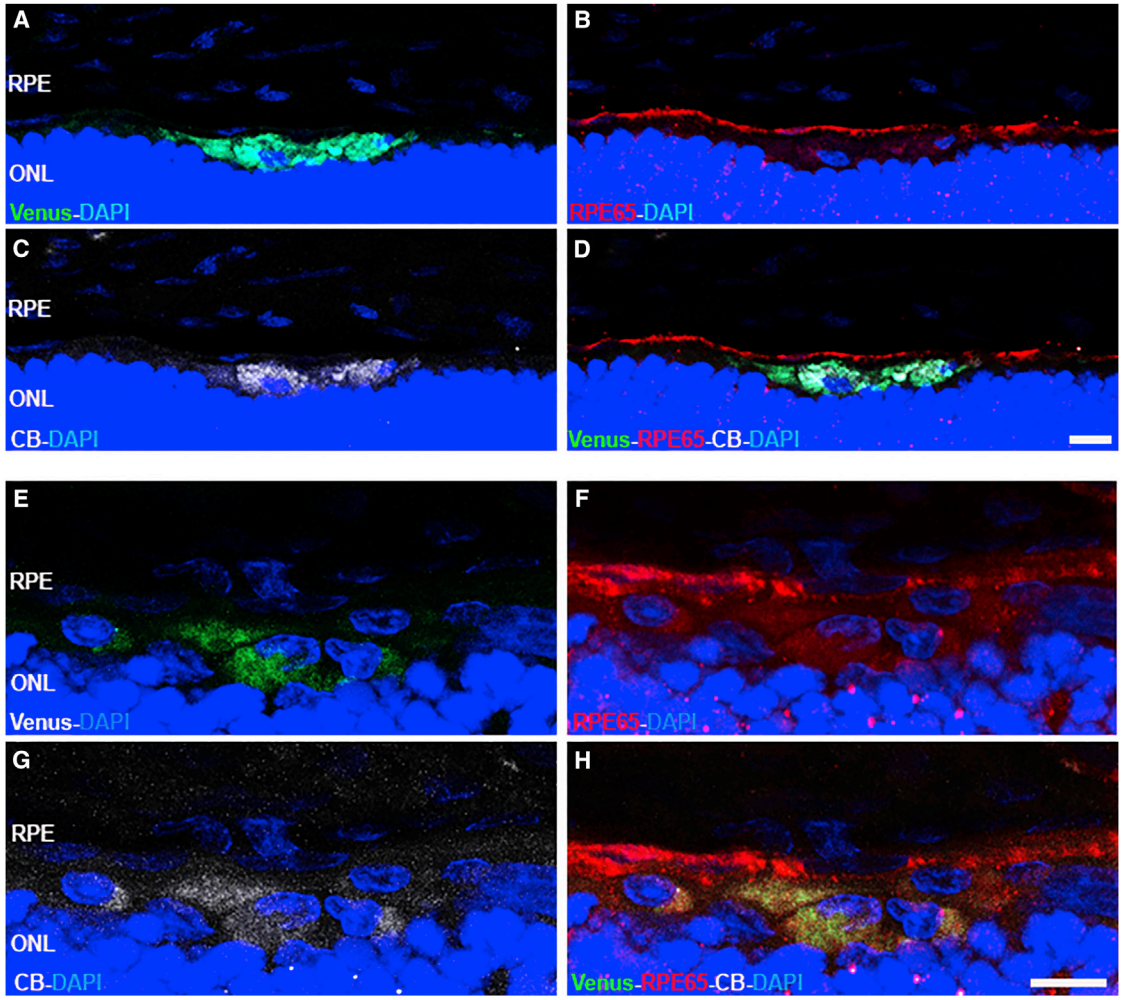

Figure 5. Injected Cell Location

(A–H) Representative fluorescence image of the retinal cross section showing rat RPE cells transfected with Venus (green) (A and E), labeled with CellBrite (white) (C and G), and immunostained with RPE65 (red) (B, D, F, and H). Nuclei were labeled with DAPI (blue). Scale bar, 20 μm. CB, CellBrite; RPE, retinal pigment epithelium; ONL, outer nuclear layer.

does not target transcriptionally active genomic sequences.[36–38] Furthermore, the use of pFAR4 plasmids would not transfer antibiotic resistance genes into the patient, and is thus safer than other plasmids. It eliminates the risk of colonization of endogenous flora, allergic reactions in susceptible patients to antibiotics, and the risk for horizontal gene transfer that could provide pathogenic bacteria with resistance to antibiotics that are used to treat humans.[39] In our approach, ARPE-19 and primary IPE and RPE cells were transfected ex vivo, followed by transplantation into the subretinal space. The ex vivo strategy ensures that only the target cells are treated, which is a task that can be difficult using an in vivo delivery approach.

Here, we also report that the PEDF-expression RPE as well IPE cells transplanted into the subretinal space do not migrate to other layers of the retina and stay localized in the RPE layer. This is a critical issue for the treatment of nAMD because the secretion of PEDF must occur at the interface of the neural retina and Bruch's membrane to prevent the choroidal vessels from penetrating through the Bruch's membrane into the subretinal space.

In order to extend the therapeutic effect, plasmids encoding anti-angiogenic genes were delivered by nanoparticles and injected intravenously.[13] However, the frequent injections of nanoparticles might lead to systemic toxicity, making this approach unlikely to become clinically relevant. The delivery of anti-angiogenic genes by viral vectors and even the transplantation of cells transfected ex vivo using viral vectors (AAV) followed by transplantation have been demonstrated. This approach has significant side effects, such as induced innate immune response.[40–42] In addition, the high cost of vector production[43,44] coupled with other safety concerns will preclude the use of viral vectors to become clinically widespread. In contrast to viral

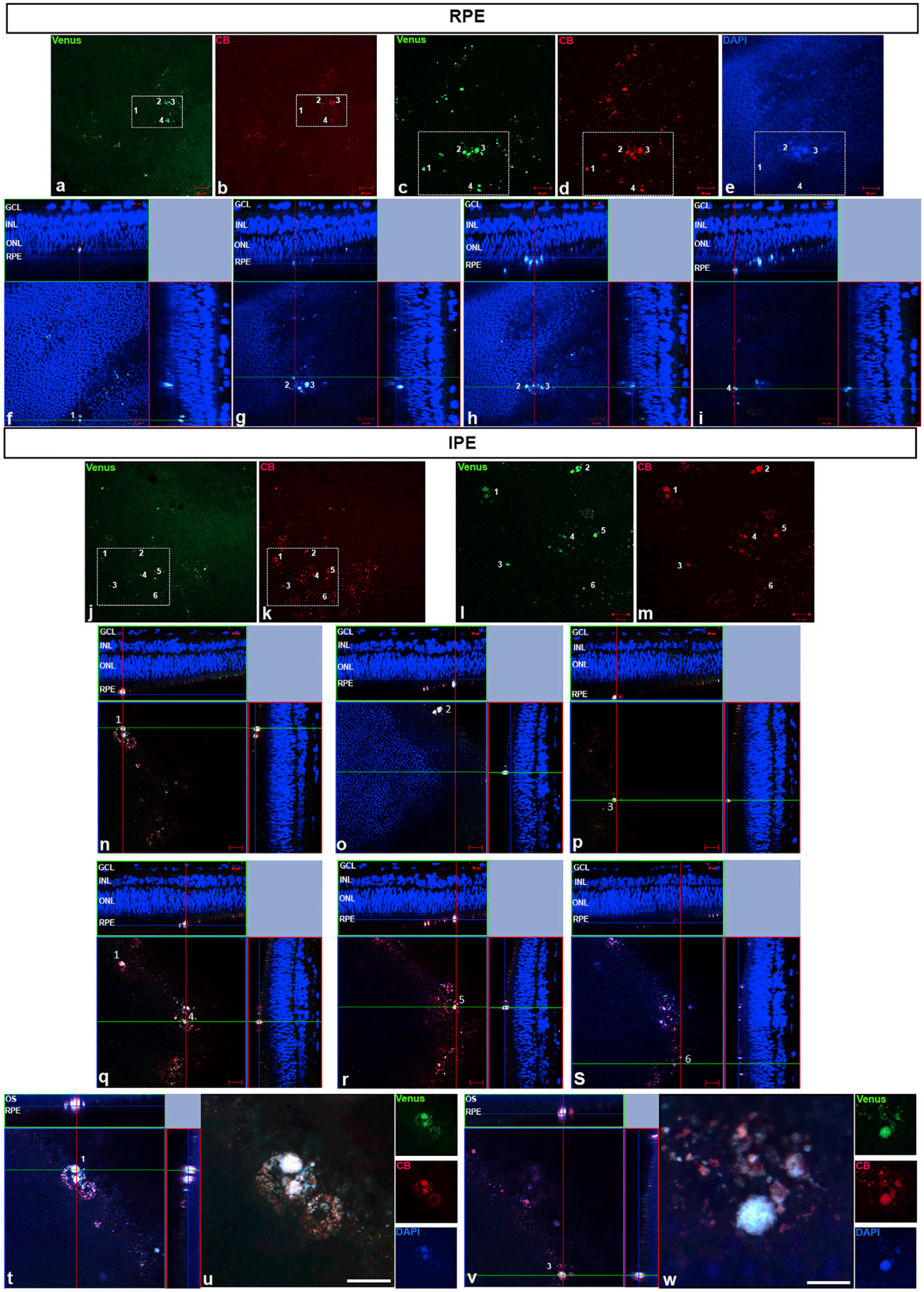

(legend on next page)

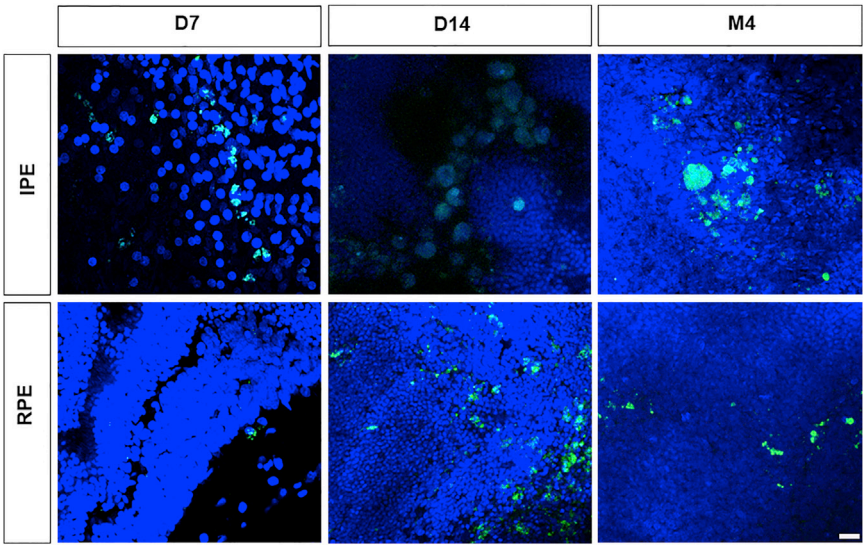

Figure 7. Long-Term Venus Expression by Transplanted Cells

Confocal images of Venus-positive cells in flat mount of retinas showing IPE and RPE cells 7 days, 15 days, and 4 months after subretinal transplantation. Scale bar, 20 μm. Nuclei were stained with TOPRO-3 (blue).

gene delivery, the *SB100X*-mediated gene delivery is relatively safe, low cost, and provides a long-lasting therapeutic effect. We have previously shown that cells engineered by the *SB100X* system secrete PEDF in culture for at least 1 year.[30] Similarly, in vivo studies have demonstrated that liver cells overexpressed the transgene for 7 months following *SB100X*-mediated delivery.[45,46]

In summary, we have shown that *SB100X*-mediated delivery of the *PEDF* gene encoded in pFAR plasmids is efficient in vitro and in vivo, even when transfecting only 5,000–30,000 pigment epithelial rat cells. The transplanted cells survived for 4 months in rats and, furthermore, *PEDF*-expressing cells transplanted to the subretinal space secrete recombinant PEDF. We also observed an inhibition of the neovascularization in a rat model of CNV. The preclinical experiments presented here aim to bring the TargetAMD consortium to its goal to conduct a phase 1 clinical trial, in which IPE cells isolated from AMD patients will be treated ex vivo with the *PEDF* gene, followed by immediate autologous subretinal transplantation.

MATERIALS AND METHODS

Cell Culture

ARPE-19 cells (ATCC, Manassas, VA) were cultured in DMEM (Sigma, St. Louis, MO) supplemented with 10% fetal bovine serum (FBS; GIBCO, Paisley, UK) and 1% penicillin/streptomycin/1% amphotericin B (GIBCO), and maintained in a humidified atmosphere of 95% air and 5% CO_2 at 37°C. The medium was changed three times a week, and cells were passaged at 70%–80% confluence at a ratio of 1:3.

Isolation and Culture of Rat Primary IPE and RPE Cells

The study was performed according to the Association for Research in Vision and Ophthalmology (ARVO) Resolution on the Use of Animals in Ophthalmic and Vision Research and approved by the Ethics Committee for Animal Research of the University of Navarra (protocol approval number 023-13).

Brown Norway rats (8–15 weeks) were used to isolate IPE and RPE cells. Eyes were cut below the ora serrata, and the anterior segment and posterior eyecup were separated. In the anterior segment, the iris was separated from the ciliary body and incubated in trypsin EDTA (200 mg/L EDTA + 170,000 U Trypsin/L; Lonza, Walkersvile, MD) at 37°C for 10 min. IPE cells were isolated by gently brushing the surface with a fire-polished glass spatula. Cells were centrifuged at 1,200 rpm for 10 min and the pellet was suspended in DMEM:F-12 (ATCC) medium supplemented with 10% FBS and 1% penicillin/streptomycin/amphotericin B (Lonza; complete medium) and plated into 24-well tissue culture plates. For RPE isolation, the neural retina was removed from the posterior eyecup and the RPE/choroid complex was maintained for 3 days in complete DMEM:F-12 medium; then, RPE cells were gently dislodged by brushing with a fire-polished glass spatula. The dislodged RPE cells were centrifuged and plated following the protocol used for IPE cells. IPE and RPE culture medium was changed twice a week.

To confirm the phenotype of primary cells, ARPE-19 and RPE cells were reacted with antibody to RPE65, CRALBP, and Bestrophin-1, and IPE cells were reacted with antibody to CK18. Briefly, cells were fixed in cold methanol overnight at −20°C, rinsed, permeabilized with 0.5% Triton X-100 (Sigma) containing 0.2% sodium azide (Sigma)

Figure 6. Transfected IPE and RPE Cell Location

(A–W) Fluorescence confocal images of the injected RPE (A–I) and IPE (J–W) cells previously transfected with pFAR4-SB100X-Venus (green) and labeled with CellBrite (red). The dissociated RPE and IPE primary cells transfected with Venus (green) (A, C, J, and L) and labeled with CellBrite (red) (B, D, K, and M) were transplanted in the subretinal space near to the RPE. The areas with primary cells are organized (white squares in A, B, J, and K) (scale bar, 50 μm) and detailed in images (C–E, L, and M) (scale bar, 20 μm). Upper panel: RPE-transfected cells are identified in four groups represented in different orthogonal projection confocal images (F–I). Lower panel: IPE-transfected cells are identified in six groups represented in different orthogonal projection confocal images (N–S). IPE-transfected cells numbered 1 and 3 are shown in detail (scale bar, 20 μm) in orthogonal projections (T and V) and at higher magnification by the super-resolution technique (U and W). DAPI: nuclei in blue. CB, CellBrite; GCL, ganglion cell layer; INL, inner nuclear layer; ONL, outer nuclear layer.

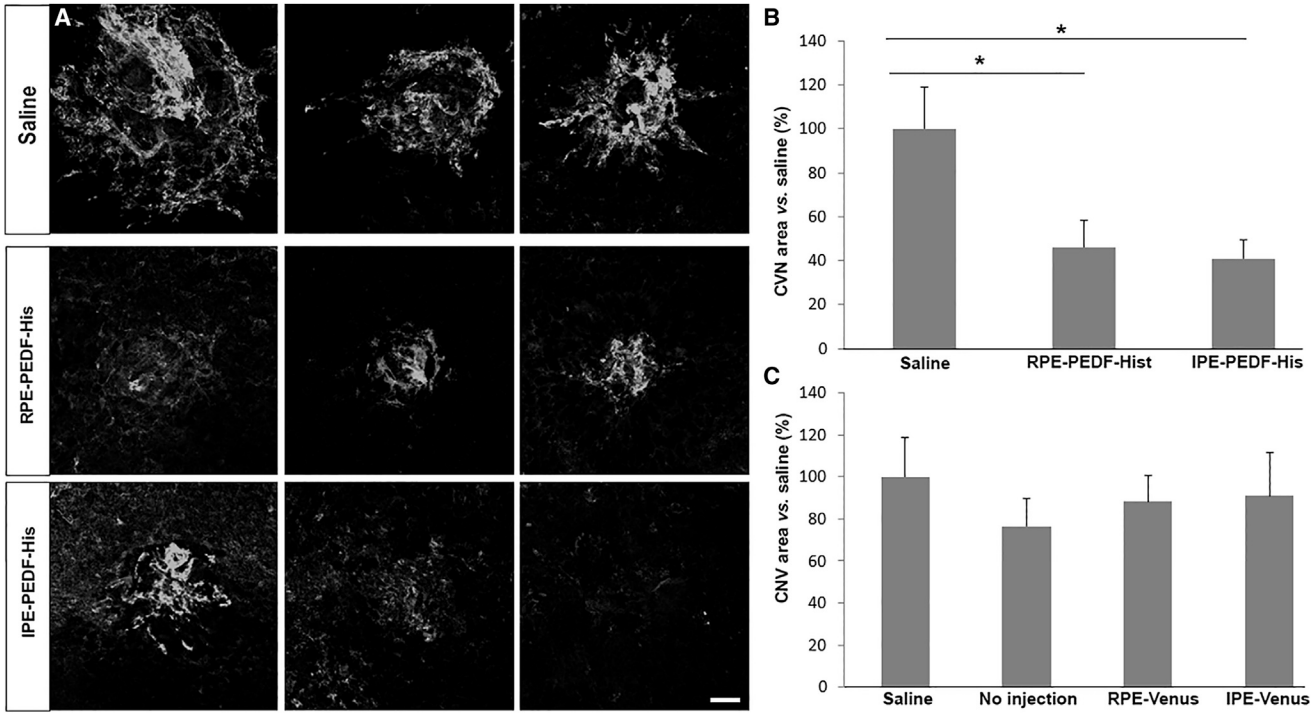

Figure 8. Effect of PEDF-Transfected Rat RPE and IPE Cells on Neovascularization in a Rat Model of Choroidal Neovascularization

Photographs and measurement of CNV area of laser-induced CNV 10 days after treatment with an injection of 5 μL of saline, transplantation with 20,000 PEDF-transfected RPE cells, and 10,000 PEDF-transfected IPE cells. (A) Photographs of lesions. Each row represents 3 different CNV lesions from 3 different animals. Vessels were stained with Caveolin-1 (white). (B and C) Measurement of CNV area. The CNV area in rats transplanted with PEDF-transfected cells is approximately 50% less than that of the saline control ($p < 0.05$) (B). CNV area of control groups (C). There was no statistical difference among control groups. Area of CNV was calculated using Fiji software, and data were presented as a percentage of mean ± SEM (n = 3) versus the saline group. Scale bar, 50 μm. *$p < 0.05$.

and 1% BSA (Sigma) for 30 min and incubated with primary antibodies: RPE65 (mouse monoclonal, ab78036, 1:100, Abcam, Cambridge, UK), Bestrophin-1 (rabbit polyclonal, orb323221, 1:250, Biorbyt, San Francisco, CA), CRALBP (rabbit polyclonal, orb182730, 1:250, Biorbyt), and CK18 (mouse monoclonal, M7010, 1:250, DAKO, Glostrup, Denmark). After overnight incubation with primary antibodies, cells were rinsed and incubated with the appropriate secondary antibody: Alexa Fluor Donkey anti-mouse, A10036, 1:250; (Invitrogen, Paisley, UK) and Alexa Fluor Donkey anti-rabbit, A21206, 1:250 (Invitrogen). DAPI (H1200, Vector) was used to label nuclei.

Construction and Production of pFAR4 Derivatives

To construct the pFAR4-ITRs CMV PEDF BGH and pFAR4-ITRs CMV PEDF-His BGH plasmids, relevant sequences (CMV-PEDF, CMV-PEDF-His, and BGH) were amplified by PCR using pT2-CMV-PEDF/EGFP[27] as a template. This latter plasmid carries a human *PEDF* cDNA that was generated from ARPE-19 cells (ATCC). The PCR fragments were then inserted stepwise into pFAR4-ITRs, which is a pFAR4 derivative carrying the ITR sequences amplified from pT2/BH (a gift from Perry Hackett [Addgene plasmid # 26556, Addgene, Cambridge, MA]). pFAR4 is a miniplasmid vector that is devoid of antibiotic resistance genes.[39] The expression cassette CMV-SB100x-SV40 was excised from pCMV (CAT)T7-SB100x[47] and introduced into pFAR4, resulting in pFAR4-CMV-SB100X-SV40. Similarly, the DNA sequence encompassing CAGGS-Venus-SV40 flanked by both ITRs was excised from pT2-CAGGS-Venus[47] and introduced into the pFAR4 vector, resulting in pFAR4-ITRs-CAGGS Venus.

All pFAR4 constructs were constructed and propagated using a dedicated bacterial strain (TM # 47-9a) that allows plasmid production in the absence of antibiotics.[39] Plasmids were purified using Endofree plasmid preparation kits (Macherey Nagel, Hoerdt, France). Plasmid integrity and endotoxin levels were assessed using standard and LAL (Limulus Amoebocyte Lysate, Lonza) procedures, respectively.

Transfection of ARPE-19 and Primary Cells

All transfections were carried out by electroporation with the Neon Transfection System using the 10-μL kit (Invitrogen) following the manufacturer's protocol. Briefly, 2,000–20,000 cells were suspended in 11 μL of buffer R and mixed with 2 μL of plasmid mixture (total DNA concentration of 500 ng) and electroporated. The ratio of plasmid to *SB100X* used was 1:16. Electroporation parameters for ARPE-19 cells were 1350 V, 20 ms, and 2 pulses, and electroporation parameters for primary RPE and IPE cells were 1,100 V, 20 ms, and 2 pulses.

Transfected cells were plated in 96-well plates. After electroporation, cells were cultured for 3 days in antibiotic-free DMEM:F-12 medium.

Quantification of PEDF by ELISA

To evaluate PEDF accumulation over 72 hr, 30,000 ARPE-19, primary rat RPE, and primary rat IPE cells transfected with pFAR4-CMV-PEDF or pFAR4-Venus were seeded in 96-well plates with a first change of medium after 3 days; PEDF accumulation was quantified during the following 3 days in the cell culture medium at 24, 48, and 72 hr. Phase contrast images were acquired before the cell cultures were terminated.

To determine PEDF secretion, 30,000 *PEDF*-transfected ARPE-19, primary rat RPE, and primary rat IPE cells were seeded in 96-well plates and PEDF secretion during 72 hr was quantified by ELISA at 3, 6, 9, 12, 15, 21, 28, and 56 days after transfection.

PEDF in culture medium was quantified by ELISA (DuoSet Human SerpinF1/PEDF Kit; R&D Systems, Abingdon, UK) according to the manufacturer's protocol. Sample dilution for ARPE-19 cells was 1:5,000 and 1:100 for primary IPE and RPE cells.

PEDF Detection by Western Blot

PEDF protein expression and secretion was analyzed by western blot as previously reported.[48,49] A volume of 7.5 µL was loaded on the gels, and loading was verified by Ponceau S red staining. To visualize PEDF, blots were reacted with monoclonal anti-PEDF antibody (PEDF [mouse monoclonal, MAB1059, 1:1,000, Chemicon, Temecula, CA]) followed by horseradish peroxidase-conjugated goat anti-mouse antibody (sc2005; 1:10,000, Santa Cruz Biotechnology, Dallas, TX).

Localization of IPE and RPE Cells Transplanted Subretinally

Ten thousand primary IPE, RPE, or ARPE-19 cells were transplanted to the subretinal space of rats; for localization of the transplanted cells and evaluation of cell survival, rats were euthanized by cervical dislocation 7 days, 15 days, or 4 months after cell transplantation. Cells were transfected with pFAR4-Venus when the objective was cell localization and with pFAR4-CMV-PEDF-His to visualize PEDF production by immunofluorescence.

Eyes for histological staining or immunological analysis in tissue sections were fixed in 4% paraformaldehyde (PFA) for 1 hr, transferred into 30% sucrose for 24 hr prior to embedding in OCT compound (Tissue TeK, Sakura, Alphen aan den Rijn, Netherlands), and stored at −20°C until use. Samples were sectioned in 12- to 14-µm sections with a cryostat (HM520 Microm) and collected on "superfrost plus" glass slices (Thermo, Braunshweig, Germany). Slides were stored at −20°C until used. Slides stained with nuclear markers, DAPI (Vector) or TOPRO-3 (T3605, Life Technologies, Carlsbad, CA), were observed and photographed with a fluorescence (Axio Imager M1, Zeiss, Oberkochen, Germany) or confocal (LSM510 and LSM800; Zeiss) microscope.

Eyes to be analyzed in a flat mount were enucleated, and the choroid-RPE complex was fixed in 4% PFA for 1 hr at 4°C, rinsed with PBS, and flat mounted in a cross. Samples were then stained with TOPRO-3 or DAPI and visualized by confocal microscope. For immunostaining, flat mounts were permeabilized with 0.25% Triton X-100 and 1% BSA for 30 min. Anti-PEDF (mouse monoclonal, MAB1059, 1:1,000, Chemicon), anti-Histidine (6-His, goat polyclonal, NBP1-25939, 1:400, Novus, Cambridge, UK), and zonula occludens with Alexa 594 (ZO-1, mouse monoclonal, 1364021A, 1:100, Invitrogen) antibodies were used for immuno-localization. After rinsing in PBS, flat mounts were incubated with the appropriate secondary antibodies (Alexa Fluor Donkey anti-mouse 488, A21202, 1:250 for PEDF and Alexa Fluor Donkey anti-Goat 594, A11058, 1:250 for 6-His) and counterstained with a nuclear marker (DAPI or TOPRO-3). A confocal microscope (LSM510 and LSM800 with Airyscan; confocal super-resolution imaging, Zeiss) was used to acquire immunofluorescence images and orthogonal projections over the z plane.

In order to be sure the injected and observed RPE and IPE cells were the transfected cells, we stained the primary cells in culture with an infrared (647 nm) CellBrite dye (Cytoplasmic Membrane Labeling Kit, 1:200; Biotium, Hayward, CA), which labels cell cytoplasmic membranes and organelles. For the CellBrite staining, 1 mL was mixed in 10^6 RPE and IPE cells in DMEM-F12 supplemented with 10% FBS. The medium was removed, and the cells were rinsed with PBS and incubated for 40 min under cell culture conditions in the staining solution. Then, the cells were centrifuged three times at 1,200 rpm during 10 min and rinsed with PBS three times, and fresh medium was added before the injection procedure.

Laser-Induced CNV Model and Subretinal Cell Transplantation

Brown Norway male rats (8–10 weeks) were anesthetized, and eyes were dilated with a mixture of phenylephrine (7.8 mg/mL) and tropicamide (3 mg/mL) eye drops. Four laser photocoagulation spots (250-mW intensity, 0.05 s, and 75-µm spot size) were made concentrically around the optic nerve using a coverslip as a contact lens. Rupture of Bruch's membrane was confirmed by bubble formation. Laser rupture sites with hemorrhage or subretinal bleeding at the time of laser application were excluded from analysis.[50]

To evaluate the efficacy of the treatment, 2 days after inducing CNV, 10,000 IPE or 20,000 RPE cells transfected with pFAR4-CMV-PEDF-His were transplanted subretinally. For subretinal transplantation, rats were anesthetized by intraperitoneal administration of a mixture of ketamine (Imalgene 1000, Merial laboratories, Barcelona, Spain; 75 mg/kg) and xylazine (Xilagesic 2%, Calier laboratories, Barcelona, Spain; 10 mg/kg). For transplantation, pupils were dilated, eyes were anesthetized with a double anesthetic (Tetracaine chlorohydrate 1 mg/10 mL and oxibuprocaine chlorohydrate 4 mg/10 mL; Alcon cusí, Barcelona, Spain) and stabilized using a suture, and the superior conjunctiva and subconjunctival tissue was cut to expose the sclera. A hole was made into the subretinal space using a 27G needle, and the appropriate number of cells suspended in 5 µL of PBS was infused using a 25G de Juan cannula (Synergetics, O'Fallon, MO) attached to a 25-µL Hamilton syringe (Hamilton Messtchnik, Höchst, Germany). The scleral wound was not sutured; oxytetracycline ointment

(Terramicina; Farmasierra laboratories, Madrid, Spain) was applied to the wound. In this experiment, six groups of 3 rats each were treated as follows: 3 rats were transplanted with 10,000 IPE cells transfected with the Venus gene, 3 rats were transplanted with 10,000 IPE cell transfected with the *PEDF-His* gene, 3 rats were transplanted with 20,000 RPE cells transfected with the Venus gene, 3 rats were transplanted with 20,000 RPE cells transfected with the *PEDF-His* gene, 3 rats were transplanted with saline, and 3 rats served as non-transplanted controls.

Ten days after cell transplantation, rats were euthanized and the RPE/choroid complex was processed for analysis in flat mount following the protocol described above for caveolin-1 immunostaining. The CNV area in retinal flat mounts was identified with caveolin-1 staining (Rabbit polyclonal, #3238, 1:400, Cell Signaling, Leiden, Netherlands), followed by reaction with secondary antibody Alexa Fluor Goat anti-Rabbit 488 (A11008, 1:250; Invitrogen). Flat mounts were photographed using a confocal microscope to obtain a single image. The CNV areas were quantified with Fiji software (a distribution of ImageJ) V1.48q by 2 investigators who were blinded to the study groups.

Statistical Analysis

Data are presented as mean ± SEM. Statistical analysis was performed using the SPSS 20 program (SPSS, Chicago, IL). In vitro studies were analyzed by using an ANOVA for repeated measurements; a one-way ANOVA with Bonferroni and Dunnett's post hoc tests was performed for the CNV area results after confirming the normal distribution of the data.

SUPPLEMENTAL INFORMATION

Supplemental Information includes five figures and can be found with this article online at http://dx.doi.org/10.1016/j.omtn.2017.08.001.

CONSORTIUM

Other members of the TargetAMD consortium are Nina Harmening (UNIGE), Argyrios Chronopoulos (UNIGE), Helena Escobar (MDC), Csaba Miskey (PEI), Attila Sebe (PEI), Anna Dalda (PEI), Mattia Ronchetti (IGEA), Claudio Bertacchini (IGEA), Giacomo Perazzolo Gallo (IGEA), Ruggero Cadossi (IGEA), Goran Petrovski (UD-G), Zoltan Vereb (UD-G), Gábor Zahuczky (UD-G), Pablo Aranda (3P), Verónica Fernández (3P), Edita Mistinie (3P), Jaime Vaquerizo (3P), Dámaso Molero Sánchez (3P), Muriel Audit, (GenoSafe), Séverine Pouillot, (GenoSafe), Stéphane Roques (GenoSafe), Susanne Binder (KAR), Kerstin Steindl (KAR), Joost H. van den Berg (AmBTU), Bastiaan Nuijen (AmBTU), Maaike van Zon (AmBTU), Jos H. Beijnen (AmBTU), Anna Dobias (UKA), and Antje Schiefer (UKA).

AUTHOR CONTRIBUTIONS

Conceptualization: A.G.-L., P.F.-R., F.P., M.H., S.R., and L.G.-G.; Data Curation: L.G.-G., M.H., J.B., S.R., and P.F.-R.; Funding Acquisition: G.T., A.G.-L., P.F.-R., D.S., Z. Izsvák, Z. Ivics, F.P., and S.J.; Investigation: L.G.-G., S.R., M.H., J.B., P.F.-R., and M.K.; Methodology: S.D., M.K., C.M., J.B., and J.R.R.-M.; Resources: Z. Izsvák, Z. Ivics, D.S., and C.M.; Supervision: A.G.-L., P.F.-R., F.P., and G.T.; Writing – Original Draft: L.G.-G., S.R., M.H., and P.F.-R.; Writing – Review and Editing: G.T., A.G.-L., P.F.-R., C.M., D.S., Z. Izsvák, Z. Ivics, J.R.R., F.P., and S.J.

CONFLICTS OF INTEREST

Z. Izsvák and Z. Ivics are co-inventors on several patents on *Sleeping Beauty* transposon technology.

ACKNOWLEDGMENTS

This project has received funding from the European Union's Seventh Framework Programme for research, technological development and demonstration under grant agreement number 305134 (TargetAMD). L.G.-G. received a predoctoral grant from the Asociación de Amigos de la Universidad de Navarra. Perry Hackett (University of Minnesota) is kindly acknowledged for the gift of pT2/BH.

REFERENCES

1. Kwak, N., Okamoto, N., Wood, J.M., and Campochiaro, P.A. (2000). VEGF is major stimulator in model of choroidal neovascularization. Invest. Ophthalmol. Vis. Sci. *41*, 3158–3164.
2. Sivaprasad, S., and Hykin, P. (2013). What is new in the management of wet age-related macular degeneration? Br. Med. Bull. *105*, 201–211.
3. Bhutto, I.A., McLeod, D.S., Hasegawa, T., Kim, S.Y., Merges, C., Tong, P., and Lutty, G.A. (2006). Pigment epithelium-derived factor (PEDF) and vascular endothelial growth factor (VEGF) in aged human choroid and eyes with age-related macular degeneration. Exp. Eye Res. *82*, 99–110.
4. Tombran-Tink, J., and Barnstable, C.J. (2003). PEDF: a multifaceted neurotrophic factor. Nat. Rev. Neurosci. *4*, 628–636.
5. Pieramici, D.J., and Avery, R.L. (2006). Ranibizumab: treatment in patients with neovascular age-related macular degeneration. Expert Opin. Biol. Ther. *6*, 1237–1245.
6. Rosenfeld, P.J., Rich, R.M., and Lalwani, G.A. (2006). Ranibizumab: phase III clinical trial results. Ophthalmol. Clin. North Am. *19*, 361–372.
7. Kovach, J.L., Schwartz, S.G., Flynn, H.W., Jr., and Scott, I.U. (2012). Anti-VEGF treatment strategies for wet AMD. J. Ophthalmol. *2012*, 786870.
8. Kwong, T.Q., and Mohamed, M. (2014). Anti-vascular endothelial growth factor therapies in ophthalmology: current use, controversies and the future. Br. J. Clin. Pharmacol. *78*, 699–706.
9. Dakin, H.A., Wordsworth, S., Rogers, C.A., Abangma, G., Raftery, J., Harding, S.P., Lotery, A.J., Downes, S.M., Chakravarthy, U., and Reeves, B.C.; IVAN Study Investigators (2014). Cost-effectiveness of ranibizumab and bevacizumab for age-related macular degeneration: 2-year findings from the IVAN randomised trial. BMJ Open *4*, e005094.
10. Jackson, T.L., and Kirkpatrick, L. (2011). Cost comparison of ranibizumab and bevacizumab. BMJ *343*, d5058.
11. Haddock, L.J., Ramsey, D.J., and Young, L.H. (2014). Complications of subspecialty ophthalmic care: endophthalmitis after intravitreal injections of anti-vascular endothelial growth factor medications. Semin. Ophthalmol. *29*, 257–262.
12. Krishnan, R., Goverdhan, S., and Lochhead, J. (2009). Submacular haemorrhage after intravitreal bevacizumab compared with intravitreal ranibizumab in large occult choroidal neovascularization. Clin. Experiment. Ophthalmol. *37*, 384–388.
13. Luo, L., Zhang, X., Hirano, Y., Tyagi, P., Barabás, P., Uehara, H., Miya, T.R., Singh, N., Archer, B., Qazi, Y., et al. (2013). Targeted intraceptor nanoparticle therapy reduces angiogenesis and fibrosis in primate and murine macular degeneration. ACS Nano *7*, 3264–3275.
14. Maclachlan, T.K., Lukason, M., Collins, M., Munger, R., Isenberger, E., Rogers, C., Malatos, S., Dufresne, E., Morris, J., Calcedo, R., et al. (2011). Preclinical safety

evaluation of AAV2-sFLT01- a gene therapy for age-related macular degeneration. Mol. Ther. *19*, 326–334.

15. Zhang, X., Das, S.K., Passi, S.F., Uehara, H., Bohner, A., Chen, M., Tiem, M., Archer, B., and Ambati, B.K. (2015). AAV2 delivery of Flt23k intraceptors inhibits murine choroidal neovascularization. Mol. Ther. *23*, 226–234.
16. Lambert, N.G., Zhang, X., Rai, R.R., Uehara, H., Choi, S., Carroll, L.S., Das, S.K., Cahoon, J.M., Kirk, B.H., Bentley, B.M., et al. (2016). Subretinal AAV2.COMP-Ang1 suppresses choroidal neovascularization and vascular endothelial growth factor in a murine model of age-related macular degeneration. Exp. Eye Res. *145*, 248–257.
17. Campochiaro, P.A., Nguyen, Q.D., Shah, S.M., Klein, M.L., Holz, E., Frank, R.N., Saperstein, D.A., Gupta, A., Stout, J.T., Macko, J., et al. (2006). Adenoviral vector-delivered pigment epithelium-derived factor for neovascular age-related macular degeneration: results of a phase I clinical trial. Hum. Gene Ther. *17*, 167–176.
18. Li, F., Zeng, Y., Xu, H., and Yin, Z.Q. (2015). Subretinal transplantation of retinal pigment epithelium overexpressing fibulin-5 inhibits laser-induced choroidal neovascularization in rats. Exp. Eye Res. *136*, 78–85.
19. Rivière, C., Danos, O., and Douar, A.M. (2006). Long-term expression and repeated administration of AAV type 1, 2 and 5 vectors in skeletal muscle of immunocompetent adult mice. Gene Ther. *13*, 1300–1308.
20. Heier, J.S., Kherani, S., Desai, S., Dugel, P., Kaushal, S., Cheng, S.H., Delacono, C., Purvis, A., Richards, S., Le-Halpere, A., et al. (2017). Intravitreous injection of AAV2-sFLT01 in patients with advanced neovascular age-related macular degeneration: a phase 1, open-label trial. Lancet *390*, 50–61.
21. Campochiaro, P.A., Lauer, A.K., Sohn, E.H., Mir, T.A., Naylor, S., Anderton, M.C., Kelleher, M., Harrop, R., Ellis, S., and Mitrophanous, K.A. (2017). Lentiviral vector gene transfer of endostatin/angiostatin for macular degeneration (GEM) study. Hum. Gene Ther. *28*, 99–111.
22. Yant, S.R., Meuse, L., Chiu, W., Ivics, Z., Izsvak, Z., and Kay, M.A. (2000). Somatic integration and long-term transgene expression in normal and haemophilic mice using a DNA transposon system. Nat. Genet. *25*, 35–41.
23. Walisko, O., Schorn, A., Rolfs, F., Devaraj, A., Miskey, C., Izsvák, Z., and Ivics, Z. (2008). Transcriptional activities of the *Sleeping Beauty* transposon and shielding its genetic cargo with insulators. Mol. Ther. *16*, 359–369.
24. Hudecek, M., Izsvák, Z., Johnen, S., Renner, M., Thumann, G., and Ivics, Z. (2017). Going non-viral: the *Sleeping Beauty* transposon system breaks on through to the clinical side. Crit. Rev. Biochem. Mol. Biol. *52*, 355–380.
25. Zayed, H., Izsvák, Z., Walisko, O., and Ivics, Z. (2004). Development of hyperactive *Sleeping Beauty* transposon vectors by mutational analysis. Mol. Ther. *9*, 292–304.
26. Izsvák, Z., Ivics, Z., and Plasterk, R.H. (2000). *Sleeping Beauty*, a wide host-range transposon vector for genetic transformation in vertebrates. J. Mol. Biol. *302*, 93–102.
27. Johnen, S., Izsvák, Z., Stöcker, M., Harmening, N., Salz, A.K., Walter, P., and Thumann, G. (2012). *Sleeping Beauty* transposon-mediated transfection of retinal and iris pigment epithelial cells. Invest. Ophthalmol. Vis. Sci. *53*, 4787–4796.
28. Thumann, G., Harmening, N., Prat-Souteyrand, C., Marie, C., Pastor, M., Sebe, A., Miskey, C., Hurst, L.D., Diarra, S., Kropp, M., et al. (2017). Engineering of PEDF-expressing primary pigment epithelial cells by the *SB* transposon system delivered by pFAR4 plasmids. Mol. Ther. Nucleic Acids *6*, 302–314.
29. Petrus-Reurer, S., Bartuma, H., Aronsson, M., Westman, S., Lanner, F., André, H., and Kvanta, A. (2017). Integration of subretinal suspension transplants of human embryonic stem cell-derived retinal pigment epithelial cells in a large-eyed model of geographic atrophy. Invest. Ophthalmol. Vis. Sci. *521*, 1314–1322.
30. Johnen, S., Djalali-Talab, Y., Kazanskaya, O., Möller, T., Harmening, N., Kropp, M., Izsvák, Z., Walter, P., and Thumann, G. (2015). Antiangiogenic and neurogenic activities of *Sleeping Beauty*-mediated PEDF-transfected RPE cells in vitro and in vivo. BioMed Res. Int. *2015*, 863845.
31. Adelman, R.A., Zheng, Q., and Mayer, H.R. (2010). Persistent ocular hypertension following intravitreal bevacizumab and ranibizumab injections. J. Ocul. Pharmacol. Ther. *26*, 105–110.
32. Carneiro, A.M., Barthelmes, D., Falcão, M.S., Mendonça, L.S., Fonseca, S.L., Gonçalves, R.M., Faria-Correia, F., and Falcão-Reis, F.M. (2011). Arterial thromboembolic events in patients with exudative age-related macular degeneration treated with intravitreal bevacizumab or ranibizumab. Ophthalmologica *225*, 211–221.
33. Thumann, G. (2012). Prospectives for gene therapy of retinal degenerations. Curr. Genomics *13*, 350–362.
34. Izsvák, Z., Chuah, M.K.L., Vandendriessche, T., and Ivics, Z. (2009). Efficient stable gene transfer into human cells by the *Sleeping Beauty* transposon vectors. Methods *49*, 287–297.
35. Belay, E., Dastidar, S., VandenDriessche, T., and Chuah, M.K.L. (2011). Transposon-mediated gene transfer into adult and induced pluripotent stem cells. Curr. Gene Ther. *11*, 406–413.
36. Izsvák, Z., Hackett, P.B., Cooper, L.J.N., and Ivics, Z. (2010). Translating *Sleeping Beauty* transposition into cellular therapies: victories and challenges. BioEssays *32*, 756–767.
37. Liu, G., Geurts, A.M., Yae, K., Srinivasan, A.R., Fahrenkrug, S.C., Largaespada, D.A., Takeda, J., Horie, K., Olson, W.K., and Hackett, P.B. (2005). Target-site preferences of *Sleeping Beauty* transposons. J. Mol. Biol. *346*, 161–173.
38. Yant, S.R., Wu, X., Huang, Y., Garrison, B., Burgess, S.M., and Kay, M.A. (2005). High-resolution genome-wide mapping of transposon integration in mammals. Mol. Cell. Biol. *25*, 2085–2094.
39. Marie, C., Vandermeulen, G., Quiviger, M., Richard, M., Préat, V., and Scherman, D. (2010). pFARs, plasmids free of antibiotic resistance markers, display high-level transgene expression in muscle, skin and tumour cells. J. Gene Med. *12*, 323–332.
40. Askou, A.L., Aagaard, L., Kostic, C., Arsenijevic, Y., Hollensen, A.K., Bek, T., Jensen, T.G., Mikkelsen, J.G., and Corydon, T.J. (2015). Multigenic lentiviral vectors for combined and tissue-specific expression of miRNA- and protein-based antiangiogenic factors. Mol. Ther. Methods Clin. Dev. *2*, 14064.
41. Hartman, Z.C., Appledorn, D.M., and Amalfitano, A. (2008). Adenovirus vector induced innate immune responses: impact upon efficacy and toxicity in gene therapy and vaccine applications. Virus Res. *132*, 1–14.
42. Yoshioka, Y., Abe, T., Wakusawa, R., Moriya, T., Mochizuki, S., Saigo, Y., Saito, T., Murata, H., Tokita, Y., Iseya, T., et al. (2006). Recombinant AAV-transduced iris pigment epithelial cell transplantation may transfer vector to native RPE but suppress systemic dissemination. Invest. Ophthalmol. Vis. Sci. *47*, 745–752.
43. Xue, X., Huang, X., Nodland, S.E., Mátés, L., Ma, L., Izsvák, Z., Ivics, Z., LeBien, T.W., McIvor, R.S., Wagner, J.E., et al. (2009). Stable gene transfer and expression in cord blood-derived CD34+ hematopoietic stem and progenitor cells by a hyperactive *Sleeping Beauty* transposon system. Blood *114*, 1319–1330.
44. Hackett, P.B., Largaespada, D.A., and Cooper, L.J. (2010). A transposon and transposase system for human application. Mol. Ther. *18*, 674–683.
45. Chung, S.I., Moon, H., Kim, D.Y., Cho, K.J., Ju, H.L., Kim, D.Y., Ahn, S.H., Han, K.H., and Ro, S.W. (2016). Development of a transgenic mouse model of hepatocellular carcinoma with a liver fibrosis background. BMC Gastroenterol. *16*, 13.
46. Turunen, T.A., Kurkipuro, J., Heikura, T., Vuorio, T., Hytönen, E., Izsvák, Z., and Ylä-Herttuala, S. (2016). *Sleeping Beauty* transposon vectors in liver-directed gene delivery of LDLR and VLDLR for gene therapy of familial hypercholesterolemia. Mol. Ther. *24*, 620–635.
47. Mátés, L., Chuah, M.K., Belay, E., Jerchow, B., Manoj, N., Acosta-Sanchez, A., Grzela, D.P., Schmitt, A., Becker, K., Matrai, J., et al. (2009). Molecular evolution of a novel hyperactive *Sleeping Beauty* transposase enables robust stable gene transfer in vertebrates. Nat. Genet. *41*, 753–761.
48. Fernandez-Robredo, P., Recalde, S., Moreno-Orduña, M., García-García, L., Zarranz-Ventura, J., and García-Layana, A. (2013). Azithromycin reduces inflammation in a rat model of acute conjunctivitis. Mol. Vis. *19*, 153–165.
49. Ivanescu, A.A., Fernández-Robredo, P., Heras-Mulero, H., Sádaba-Echarri, L.M., García-García, L., Fernández-García, V., Moreno-Orduna, M., Redondo-Exposito, A., Recalde, S., and García-Layana, A. (2015). Modifying choroidal neovascularization development with a nutritional supplement in mice. Nutrients *7*, 5423–5442.
50. García-Layana, A., Vásquez, G., Salinas-Alamán, A., Moreno-Montañés, J., Recalde, S., and Fernández-Robredo, P. (2009). Development of laser-induced choroidal neovascularization in rats after retinal damage by sodium iodate injection. Ophthalmic Res. *42*, 205–212.